

A study of Love wave devices in ZnO/Quartz and ZnO/LiTaO₃ structures

Ren-Chuan Chang^a, Sheng-Yuan Chu^{a,*}, Cheng-Shong Hong^{a,b}, Yu-Ting Chuang^a

^aDepartment of Electrical Engineering, National Cheng Kung University, Tainan, 701 Taiwan

^bDepartment of Electrical Engineering, Chienkuo Technology University, Changhua, 500 Taiwan

Available online 19 August 2005

Abstract

Love wave devices are very promising for sensing applications because of high sensitivity. In this paper, ZnO thin films doped with lithium (Li) and magnesium (Mg) were deposited on the 42°45' ST-cut quartz and 36° YX-LiTaO₃ substrates by RF magnetron sputtering technique. XRD, SEM, and AFM measurements investigated characteristics of the films. Under different conditions such as doping content, layer thickness, and substrate temperature, the phase velocity, temperature coefficient of frequency, electromechanical coupling coefficient and sensitivity of Love wave devices in ZnO/Quartz and ZnO/LiTaO₃ structures are presented. The maximum sensitivities of ZnO/Quartz and ZnO/LiTaO₃ are much higher than the SiO₂/Quartz and SiO₂/LiTaO₃ structures reported.

© 2005 Elsevier B.V. All rights reserved.

Keywords: Love wave; ST-cut quartz; 36° YX-LiTaO₃; Zinc oxide

1. Introduction

SAW devices have found wide application in sensors for detection in gas and liquid environment [1–4]. In liquid environment, Rayleigh surface waves have a displacement component perpendicular to the substrate, which exist as compressional waves leading to a strong radiation loss [5]. For this reason, shear horizontal (SH) polarized waves are preferred because they do not couple elastically with ideal liquids and make no radiation loss [1,2,4–6]. SH modes can be converted into Love modes by means of a layer acting as a guide. Love waves propagate in a layered structure consisting of a substrate and a layer on top of it. Resulting from the waveguide effect, Love waves will be very sensitive to surface perturbations and high sensitivity to surface loading can be achieved.

The condition for the existence of Love wave modes is the shear velocity of the overlay material less than that of the substrate [2]. Surface skimming bulk waves (SSBW) of ST-cut quartz [1–4,6–8,12], and leaky waves of 36° YX-LiTaO₃ [3,9–11,13–16] and 64° YX-LiNbO₃

[11,13,17,18] have been utilized as substrates. 36° YX-LiTaO₃ shows a large electromechanical coupling coefficient ($K^2=4.7\%$), shear velocity (4112 m/s) [11] and negative temperature coefficient of frequency (TCF) [18]. 42°45' ST-cut quartz has relatively high TCF of about +30 ppm/°C [3], low K^2 (0.11%) [1] and faster shear velocity (5060 m/s) [2,4]. Fused silica (SiO₂) [3,6,11–13], and polymethyl-methacrylate (PMMA) [16] are relatively used for the guiding layer. However, PMMA shows high acoustic losses as well as poor chemical and temperature resistance [2,3]. Until now, many papers have reported SiO₂ with a positive TCF value [18] on 36° YX-LiTaO₃ to improve TCF or on 90° rotated ST-quartz to increase K^2 . But such devices presented lower sensitivity. On the other hand, zinc oxide (ZnO) has low acoustic absorption, low loss, and high chemical, mechanical and thermal stability. Besides, the shear velocity of ZnO (2747 m/s) [1] is lower than that of SiO₂ (2850 m/s) [2] making it suitable candidate for the guiding layer. Therefore, ZnO layers with a negative TCF value [19] deposited on ST-cut quartz and LiTaO₃ were expected to compensate TCF, and increase K^2 and sensitivity.

In this paper, we investigate the effect of the substrate temperature on the properties of Li–Mg doped ZnO films on 42°45' ST-cut quartz and 36° YX-LiTaO₃ substrates by

* Corresponding author. Tel.: +886 6 2757575x62381; fax: +886 6 2345482.

E-mail address: chusy@mail.ncku.edu.tw (S.-Y. Chu).

RF magnetron sputtering technique. Besides, under different conditions, the characterization of Love wave devices in ZnO/Quartz and ZnO/LiTaO₃ structures are presented.

2. Experimental details

The Love wave devices were fabricated on 12 mm × 13 mm and 0.5 mm thick 42°45' ST-cut quartz and 0.35 mm thick 36° YX-LiTaO₃ substrates. The Inter-Digital Transducer (IDT) was patterned between the substrate and the guiding layer. The input and output IDTs consisted of 15 finger pairs with 10 μm width of electrode and 10 μm separation. The IDT center-to-center separation was 4.6 mm with an aperture of 4 mm. The IDTs were made of 200 nm aluminum. A HP 8714ES network analyzer (Agilent Technologies, Palo Alto, CA) was used for device characterization.

As a guiding layer, ZnO thin films were deposited on the top of IDT by RF magnetron sputtering using an Li–Mg doped ZnO (99.9%) target. Sputtering was carried out in argon and oxygen mixed gas atmosphere at RF power of 60 W with a chamber pressure of 10 mTorr. The deposition rates ranged from 0.43 to 0.46 μm/h. The substrate was heated to attain the desired deposition temperature. The crystallographic study of the ZnO films was confirmed by X-ray diffraction (XRD) using Cu Kα (λ=0.154 nm) radiation with a Siemens D-5000 diffractometer operated at 40 kV and 40 mA. The microstructure was observed by field emission scanning electron microscopy (FESEM) with a Hitachi S-4100 microscope and atomic force microscopy (AFM) with an NT-MDT P7LS microscope.

3. Results

3.1. XRD analysis

Fig. 1 shows X-ray diffractograms of the sputtered ZnO films as function of substrate temperature. All of the films almost show a pronounced 34.42° corresponding to (002) peak of JCPDS file 36-1451 for ZnO structure, indicative of preferential orientation with the *c*-axis. The ST-cut quartz and 36° LiTaO₃ substrates show, respectively, 26.75° and 23.73° corresponding to (101) peak of JCPDS file 83-2466 and (012) peak of JCPDS file 71-0951. It is found that the films on ST-cut quartz and LiTaO₃ formed at 100 °C both have a stronger *c*-axis orientation, and the intensity decreases as the substrate temperature is increased. Many reports indicate suitable substrate temperature enhances the film formation, especially high temperature. However, our experimental results reflect that better crystallite structure tends to be formed in cooler substrate temperature. Although the temperature is only 100 °C, the condition provides enough energy to make it possible to have good crystalline orientation. At higher temperature, the peak intensity decreases because too much energy results in

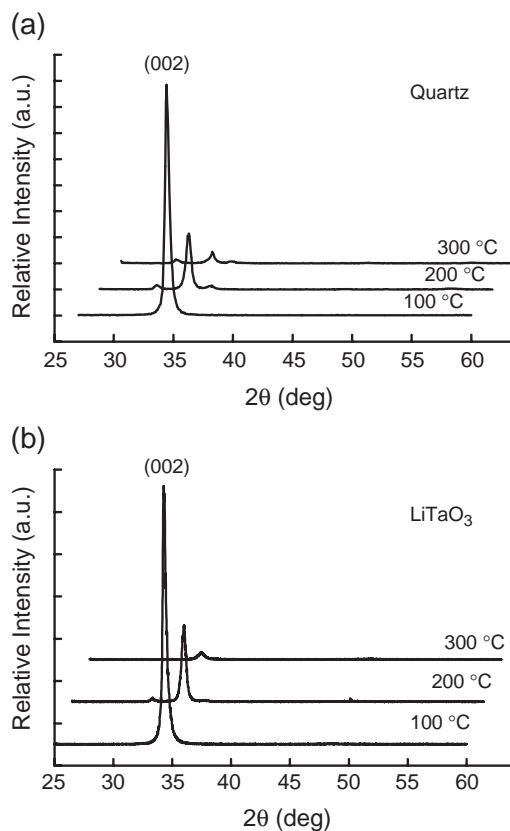


Fig. 1. X-ray diffractograms of the sputtered ZnO films on (a) 42°45' ST-cut quartz and (b) 36° YX-LiTaO₃ as function of substrate temperature.

growth and appearance of random orientations, such as (100) and (101) peaks seen at 200 and 300 °C.

Table 1 indicates the variation of ZnO films with respect to substrate temperature. The nearly FWHM values of *c*-axis orientation on quartz, 0.46° at 100 °C and 0.47° at 200 °C, reveal that the crystal qualities of the thin films are similar. And then the crystal quality becomes poor as the temperature is increased beyond 200 °C. On the side, the FWHM of the films on LiTaO₃ increases from 0.35° to 0.64° with the increase at substrate temperature. It also reveals that the degree of crystallinity of the films is deteriorated gradually.

The stress is composed of a thermal stress and an intrinsic stress. The thermal mismatch between the films and substrate results in the thermal stress due to the difference in the thermal expansion coefficients (α) of the films and substrate [20]. The intrinsic stress is due to the accumulating effect of crystallographic flows, which are built into the films during deposition process by reflected atoms, energetic argon and oxygen atoms [21]. The stress is calculated by the formula according to Ref. [22].

As shown in Table 1, a strong planar compressive stress (– sign) exists in ZnO films at 100 °C on two kinds of substrates. As the substrate temperature increase, the compressive stress becomes relaxed, and then the stress within films deviates from the free-stress turning into the tensile stress (+ sign). On one hand, raising substrate

Table 1
The variation of ZnO films with respect to substrate temperature

Substrate temperature (°C)	2 θ (deg)	FWHM (deg)	Stress (10 ¹⁰ dyn/cm ²)	Roughness (nm)
<i>42°45' ST-cut quartz</i>				
100	34.40	0.46	-0.269	3.48
200	34.47	0.47	0.625	5.07
300	34.61	0.56	2.402	26.48
<i>36° YX-LiTaO₃</i>				
100	34.29	0.35	-1.681	5.67
200	34.40	0.41	-0.269	17.33
300	34.48	0.64	0.753	12.62

*Unstressed ZnO powder, 2 θ =34.421°.

temperature promotes the cancellation between the tensile stress of substrate and the compressive stress of film to reduce thermal stress during sputtering process. However, over-high temperature induces the tensile stress larger than compressive stress to result in stress transformation. On the other hand, the defects in the films will be decreased and the oxygen will be out-diffused caused by thermal expansion. According the results, the stress on quartz and LiTaO₃ would be relieved completely between 100 and 200 °C, and between 200 and 300 °C, respectively.

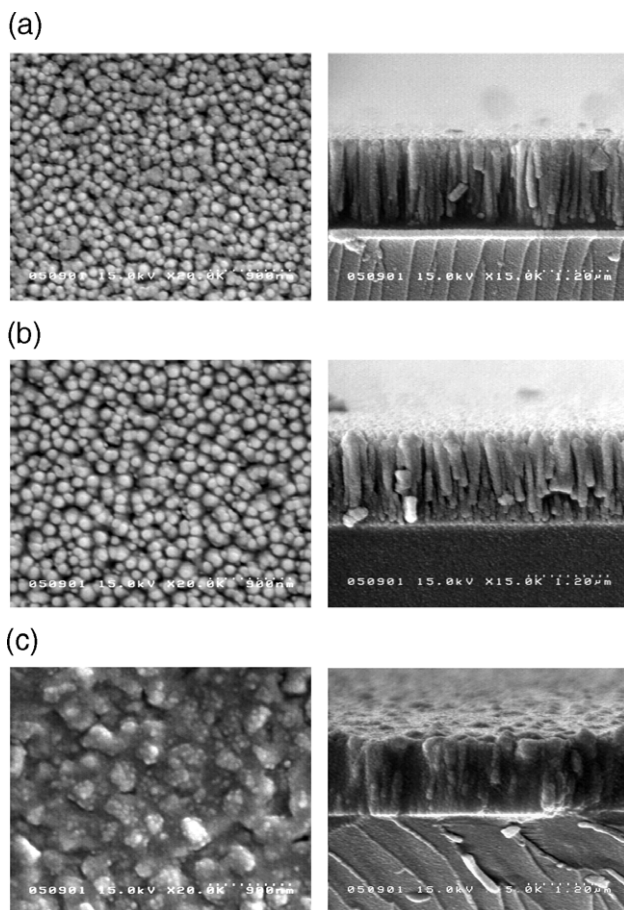


Fig. 2. The SEM images of ZnO films deposited on 42°45' ST-cut quartz at (a) 100 °C, (b) 200 °C, and (c) 300 °C (900 nm for plan-view and 1.2 μ m for cross-view).

3.2. Analysis of surface morphology

Fig. 2 displays the SEM images of ZnO films deposited on 42°45' ST-cut quartz. The temperature of substrate controls the mobility of the absorbed atoms and results in structure of deposition film. At 100 °C, the low temperature provides less kinetic energy to get smaller grains. The grains and pores are seen clearly in the plan view of Fig. 2a. As shown in the cross view image of Fig. 2a, the structure, which looks columnar, is proved to have a parallel *c*-axis orientation at 100 °C. In our experiment, a good crystallite structure tends to form at 100 °C with low mobility. When it is increasing to 200 °C, the grains seen in Fig. 2b are obviously larger than that in Fig. 2a and so are the cylindrical crystallite structures. Higher temperature provides energy of surface atoms to enhance mobility for grain growth. However, too high temperature will cause the crystallinity overgrowing. The result is seen in Fig. 2c. The grains of ZnO films rapidly grow and appear obviously in irregular shapes at the same time. The structure of *c*-axis (002) orientation becomes weaker and further almost vanishes by reason of the formation of the lateral columnar structure along the (002) direction.

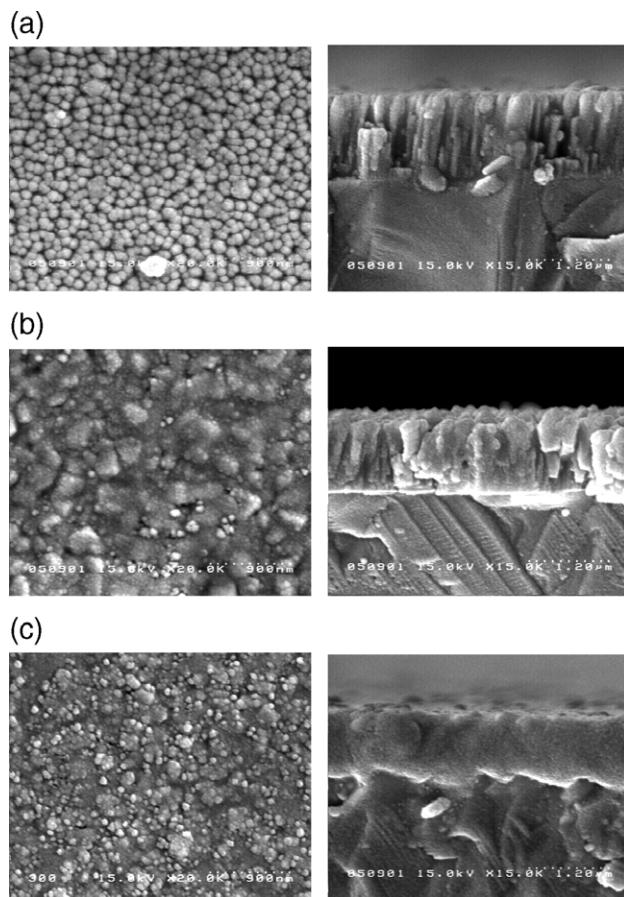


Fig. 3. The SEM images of ZnO films deposited on 36° YX-LiTaO₃ at (a) 100 °C, (b) 200 °C, and (c) 300 °C (900 nm for plan-view and 1.2 μ m for cross-view).

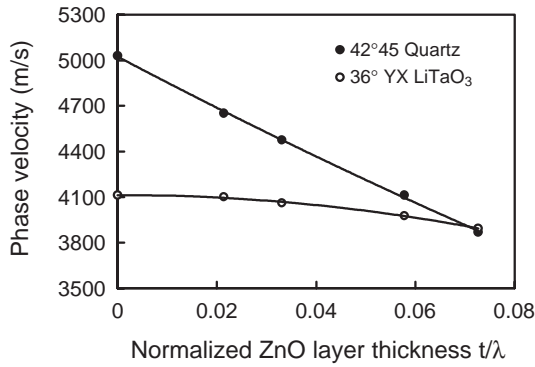


Fig. 4. Phase velocity vs. normalized layer thickness with ZnO/IDT/Quartz and ZnO/IDT/LiTaO₃ structures.

The similar condition of 36° YX-LiTaO₃ is also observed in Fig. 3. The smaller grain and better crystallite structure with *c*-axis (002) orientation are formed at 100 °C. Different from the results of quartz, the condition of the rapid growth occurs at 200 °C. When it is heated to 300 °C, the formation of the lateral columnar structure is quite significant leading to deterioration in the degree of *c*-axis crystallinity. These results coincide with XRD analysis.

The roughness (Ra) of ZnO films is shown in Table 1. The roughness of quartz increases quite slowly, whereas it increases rapidly above 200 °C, i.e. 26.48 nm of 300 °C. Over-higher temperature enhances the major growth and induces large grains with irregular shapes resulting in a rough surface [23]. Although the roughness of LiTaO₃ also varies as that of quartz, the roughness is increasing suddenly at 200 °C and slightly cutting down at 300 °C. This phenomenon could be confirmed by the SEM images in Fig. 3. The grains may overgrow and intermingle with grain boundaries. Hence, the surface deposited at 300 °C is smoother than that at 200 °C, but it remains considerably rough.

3.3. Love wave device characteristics

Phase velocity vs. normalized layer thickness with ZnO/IDT/Quartz and ZnO/IDT/LiTaO₃ structures is shown in Fig. 4. The thickness of ZnO films is measured by FESEM

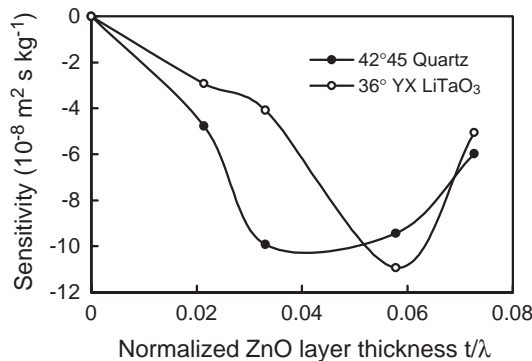


Fig. 5. Sensitivity vs. normalized ZnO layer thickness for Love wave device.

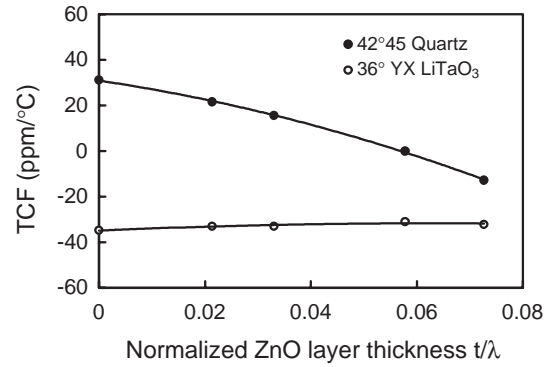


Fig. 6. Temperature coefficient of frequency vs. normalized layer thickness for Love wave device.

and with an Alpha-Step Profilometer (Surfcoeder ET-4000M). According to XRD analysis and SEM images, all of the thin films with different thicknesses show good crystal qualities. The data at zero thickness are close to the expected phase velocity in ST-cut quartz (5060 m/s) and LiTaO₃ (4112 m/s). The velocities of quartz and LiTaO₃ decrease with increasing ZnO thickness since the velocity of ZnO (2747 m/s) is smaller than the shear velocity in the substrates. The decreasing range of ZnO/IDT/Quartz is more extensive than that of ZnO/IDT/LiTaO₃.

For sensor applications, the sensitivity S_v of the relative phase velocity change $\Delta v/v$ is determined by [24]

$$S_v = \frac{\Delta v}{v} \sqrt{\frac{2}{\omega \eta \rho}}$$

where ω , η and ρ are the angular frequency, liquid viscosity and density, respectively. The difference $\Delta v/v$ is obtained by measuring the phase shift $\Delta \varphi$ [25]

$$\frac{\Delta v}{v} \approx \frac{\Delta \lambda}{2\pi L}$$

where λ and L are the wavelength and the path of propagation in the liquid, respectively, and the phase shifts were obtained by an HP 8714ES network analyzer after stable state. There is an optimum of t/λ (t is ZnO film

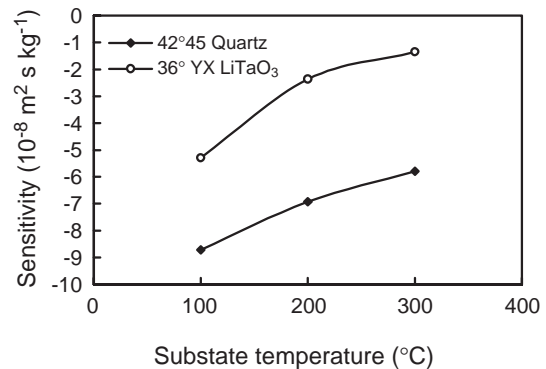


Fig. 7. The sensitivity of Love wave device as a function of substrate temperature.

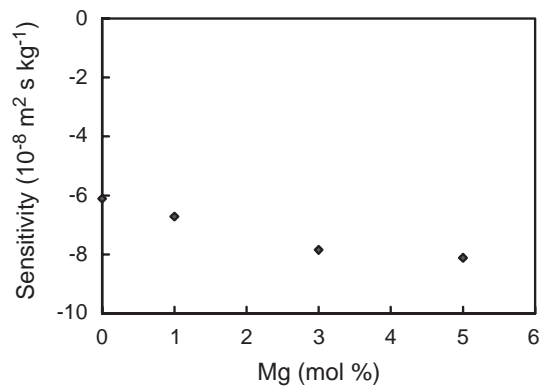


Fig. 8. Love wave device sensitivity vs. Mg-doped content.

thickness) in terms of S_v for any system. Fig. 5 shows sensitivity vs. t/λ . The sensitivity of ST-cut quartz increases with increase of layer thickness reaching the maximum at $t/\lambda=0.033$, and then decreases with increasing thickness. Because of the strong waveguiding effect, the K^2 ranges between 0.2% and 0.33%, which is larger than that in the absence of a ZnO film (0.11%) [1]. In addition, the sensitivity of LiTaO₃ also reaches the maximum at $t/\lambda=0.058$. The maximum sensitivities of ZnO/Quartz and ZnO/LiTaO₃ are, respectively, -9.93 and $-10.93 \times 10^{-8} \text{ m}^2 \text{ s/kg}$, which are much higher than the literature [3] that reported the SiO₂/Quartz ($-4.8 \times 10^{-8} \text{ m}^2 \text{ s/kg}$) and SiO₂/LiTaO₃ ($-1.8 \times 10^{-8} \text{ m}^2 \text{ s/kg}$) structures.

The TCF were calculated by substitution of center frequency for 0, 20, and 40 °C into the following equation

$$TCF = \frac{F(40^\circ\text{C}) - F(0^\circ\text{C})}{40 \times F(20^\circ\text{C})}$$

Fig. 6 shows TCF vs. t/λ for Love wave device. TCF value of ZnO/Quartz decreases with increasing film thickness and it is close to 0 ppm/°C at $t/\lambda=0.058$. TCF value of 42°45' ST-cut quartz-based Love wave devices is about +30 ppm/°C and TCF value of ZnO layer is negative [19]. An appropriate thickness of ZnO film for Love wave device can obtain the excellent TCF. However, TCF value of 36° YX-LiTaO₃-based Love wave devices is approximately in -30 to -40 ppm/°C range [11]. For this reason, TCF value of ZnO/LiTaO₃ virtually increases from -34.8 to -32.2 ppm/°C. In our experiment, the ZnO films behave insignificant effect on TCF value of ZnO/LiTaO₃ devices.

The sensitivity as a function of substrate temperature is shown in Fig. 7. The thicknesses of ZnO films are almost 1.3 μm . The sensitivities of ZnO/Quartz and ZnO/LiTaO₃ both decrease with increasing substrate temperature. Some reports indicate that rough and porous surface enhances additional mechanisms of coupling between acoustic wave and a liquid or gas motion. We could infer that too many pores and too rough surface cause extra viscosity, and they cannot compensate for the poor crystal quality of films, resulting in the deterioration in the performance of devices in liquid media.

Little literatures have been reported to improve the performance of Love wave devices by doping some components. Fig. 8 shows Love wave device sensitivity vs. Mg-doped content. It reveals preliminarily that the sensitivity is increasing a little with the increase of Mg-doping concentration from 0 mol% to 5 mol%. We may conjecture that the Mg doping with the reduction of oxygen defect [26] improves the quality and piezoelectricity of ZnO films, and leads to higher sensitivity.

4. Discussion

In our experiment, the result indicates that better crystallite structure of ZnO deposited on 42°45' ST-cut quartz and 36° YX-LiTaO₃ tends to be formed in cooler substrate temperature. The deposition of ZnO films at low substrate temperature makes it possible for applications in the flexible substrates. The intensity of *c*-axis (002) orientation and surface roughness is increasing, and the FWHM value is decreasing with the increase of substrate temperature. Love wave acoustic devices based on the ZnO/ST-cut quartz and ZnO/LiTaO₃ structures have been successfully manufactured and operated. An appropriate thickness of ZnO film for Love wave device can obtain the maximum sensitivity and excellent temperature coefficient of frequency. Higher sensitivity is also obtained at lower substrate temperature. Mg doping would raise the sensitivity a little.

Acknowledgements

This research was supported by the National Science Council of Republic of China, under Grant NSC-93-2216-E-006-033. And the authors also gratefully acknowledge the supports from Center for Micro-Nanotechnology, National Cheng Kung University.

References

- [1] S.Y. Chu, W. Water, J.T. Liaw, *Ultrasonics* 41 (2003) 133.
- [2] J. Du, G.L. Harding, J.A. Ogilvy, P.R. Dencher, M. Lake, *Sens. Actuators, A* 56 (1996) 211.
- [3] F. Herrmann, M. Weihnacht, S. Büttgenbach, *IEEE Trans. Ultrason. Ferroelectr. Freq. Control* 48 (2001) 268.
- [4] K. Kalantar-zadeh, A. Trinchì, W. Wlodarski, A. Holland, *Sens. Actuators, A* 100 (2002) 135.
- [5] W. Welsch, C. Klein, M. von Schickfus, S. Hunklinger, *Anal. Chem.* 68 (1996) 2000.
- [6] O. Tamarin, C. Déjous, D. Rebière, J. Pistré, S. Comeau, D. Moynet, J. Beziau, *Sens. Actuators, B* 91 (2003) 275.
- [7] B. Jakoby, M.J. Vellekoop, *IEEE Trans. Ultrason. Ferroelectr. Freq. Control* 45 (1998) 1293.
- [8] K. Kalantar-zadeh, Y.Y. Chen, B.N. Fry, A. Trinchì, W. Wlodarski, *IEEE Ultrason. Symp.* (2001) 353.
- [9] D.A. Powell, K. Kalantar-zadeh, S. Ippolito, W. Wlodarski, *IEEE Ultrason. Symp.* (2002) 493.

- [10] T. Shoji, K. Nakamura, D. Yamazaki, *IEEE Ultrason. Symp.* (2001) 215.
- [11] F.S. Hickernell, H.D. Knuth, R.C. Dablemont, T.S. Hickernell, *IEEE Ultrason. Symp.* (1995) 345.
- [12] B. Jakoby, M.J. Vellekoop, *Sens. Actuators, A* 68 (1998) 275.
- [13] K. Yamanouchi, H. Satoh, T. Meguro, Y. Wagatsuma, *IEEE Trans. Ultrason. Ferroelectr. Freq. Control* 42 (1995) 392.
- [14] S.J. Ippolito, S. Kandasamy, K. Kalantar-zadeh, A. Trinch, W. Wlodarski, *Sens. Lett.* 1 (2003) 33.
- [15] H. Nishiyama, N. Saito, T. Yashima, K. Sato, Y. Inoue, *Surf. Sci.* 427/428 (1999) 152.
- [16] F. Bender, R.W. Cernosek, F. Josse, *Electron. Lett.* 36 (2000) 19 (14th).
- [17] H. Yamamoto, N. Saiga, K. Nishimori, *Appl. Surf. Sci.* 169/170 (2001) 517.
- [18] S.J. Jian, S.Y. Chu, T.Y. Hung, W. Water, *J. Vac. Sci. Technol., A, Vac. Surf. Films* 22 (2004) 2424.
- [19] M. Kadota, *Jpn. J. Phys.* 36 (1997) 3076.
- [20] J.H. Jou, M.Y. Han, D.J. Cheng, *J. Appl. Phys.* 71 (1992) 4333.
- [21] W. Water, S.Y. Chu, *Mater. Lett.* 55 (2002) 67.
- [22] V. Gupta, A. Mansingh, *J. Appl. Phys.* 80 (1996) 1063.
- [23] K.B. Sundaram, A. Khan, *Thin Solid Films* 295 (1997) 87.
- [24] G. Kovacs, M.J. Vellekoop, R. Haueis, G.W. Lubking, A. Venema, *Sens. Actuators, A* 43 (1994) 38.
- [25] C.C. Tseng, *J. Appl. Phys.* 38 (1967) 4281.
- [26] S. Fujihara, C. Sasaki, T. Kimura, *J. Eur. Ceram. Soc.* 21 (2001) 2109.